Publishing House
AKAPIT

**COMPUTER METHODS IN MATERIALS SCIENCE**

Informatyka w Technologii Materiałów

**Vol. 17, 2017, No. 4**

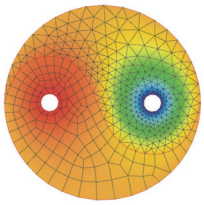

# PARALLEL FEM CODE FOR SIMULATION OF LASER DIELESS DRAWING PROCESS OF TUBES

**ANDRIJ MILENIN**

*AGH University of Science and Technology, al. Mickiewicza 30, 30-059 Kraków, Poland*
*milenin@agh.edu.pl*

**Abstract**

The present paper is devoted to the development of FEM code for simulation of laser dieless drawing process of microtubes made from magnesium alloy. Difficulties in determination parameters of such technology allowing to receive specified tube dimensions are related to the fact that this process is based on the free forming of the workpiece. The proposed solution makes use of parallel computing. The parallel solution of the vector of problems, generated by the factorial design method, was considered. The solution of this problem allows to generate acceptable window of process parameters and to determine the parameters that guarantee the required dimensions of the final pipe. A numerical efficiency of the developed code is based on the fact that all parallel processes use the same matrix, which contains addresses of non-zero elements in the stiffness matrix.

**Key words**: parallel computing, dieless drawing, metal forming, magnesium alloys

## 1. INTRODUCTION

The present paper is devoted to the process of manufacturing of the small diameter tubes using the Laser Dieless Drawing (LDD) process. Conventional dieless drawing process is based on local heating and simultaneously controlled stretching of the workpiece (Furushima & Manabe, 2007). In this process heating is usually performed using induction furnace (figure 1a). The advantage of the conventional dieless drawing is the lack of a deforming die and a large possible elongation in a single pass (for example, according to work of Kustra et al. (2016), maximum elongation is about 60% for a tube made of magnesium alloy). The disadvantage of this technology is the not controlled variability of the diameter along the tube. The LDD process is based on heating with a laser beam instead of an induction furnace (Li et al., 2002). This heating method extends the process control capabilities. For example, it is possible to obtain a pipe having a required varying diameter (Furushima et al., 2014). However, the use of laser heating leads to some difficulties. Firstly, the heat distribution becomes asymmetrical. The work of Furushima et al. (2015), suggests workpiece rotation combined with stretching to compensate the asymmetry. The concept scheme of such solution is shown in figure 1b. The second problem is the dependency of the intensity of the heating on the optical properties of the surface of the workpiece. In the presence of small dark spots on the surface of the pipe the local overheating and destruction of the material is possible. Thus, the design of the process becomes even more difficult. To solve it, the numerical simulation was used.

To analyze the dieless drawing process, FEM modeling is used quite widely. For example, in Tiernan and Hillery (2004) analyzed the drawing force. A more sophisticated analysis of dieless drawing of tubes is performed by Furushima and Manabe (2008). The authors, using the MARC/Mentat FEM program, performed an analysis of the effect of the



ISSN 1641-8581

scale factor on the temperature distribution in the thin pipes during dieless drawing. Modeling of phenomena occurring in a microscale is performed in paper (Furushima et al., 2011). In this work, using the MARC/Mentat FEM program, the Authors performed a simulation of the development of the microroughness of the pipe surface, taking into account the original inhomogeneity of the material. All of the above articles dealt with conventional dieless drawing and contained an analysis of single problems. However, none of them not addressed the problem of performing analysis based on multiple calculations, for example, determining the window of permissible process parameters or the design of the technological process. An additional complication is the difference between the dieless drawing and laser dieless drawing processes.

The model of laser dieless drawing process is much more complex than the model of the conventional process. The reasons of this are following:

1. The thermal and deformation problems become three-dimensional.
2. Boundary conditions become more complicated (because of laser heating and rotation).
3. Reduced length of the deformation zone causes an increase of the deformation gradient and sensitivity of process parameters. Additional difficulties are caused by the need to perform multiple calculations and multiscale simulations (in perspective).

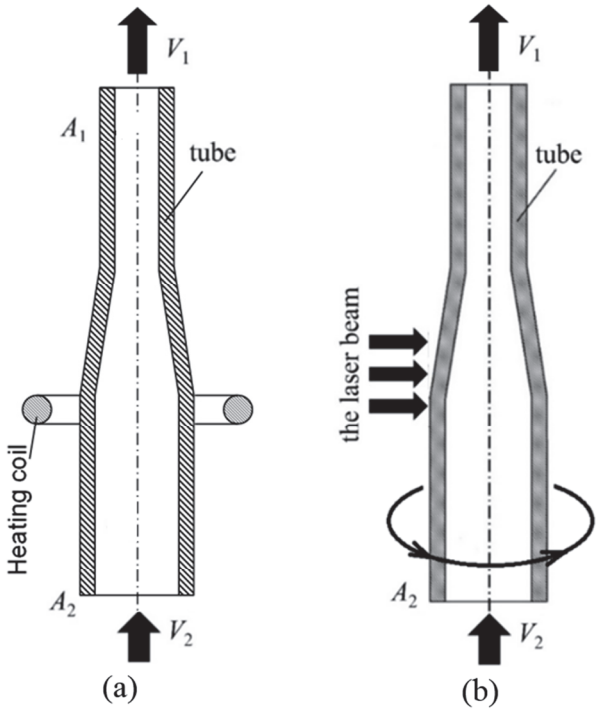


***Fig. 1.*** *Conventional (a) and laser (b) dieless drawing process of tubes.*

The solution of the problem by commercial programs is complicated due to two groups of features. The first one is related to the atypical conditions of impact to the metal. These features include the interaction with the laser beam, the possibility of fracture occurrence, the need to take into account the material properties over a wide temperature range and the workpiece rotation. This category of problems is considered in paper (Milenin et al., 2017). The second category concerns the problems of computer science and programming. The need to perform a single calculation during study of LDD process occurs very rarely. Almost always it is necessary to perform series of calculations for the purpose of calibration of the boundary conditions (for example, determination of the absorption coefficient) or to optimize and study the process. Thus, the problem to be solved is almost always an inverse problem. It is reasonable to run such calculations in parallel mode for vector of tasks. It allows to solve the inverse problem directly in the one simulation. The efficiency of this approach for the optimization of extrusion was shown in the paper (Milenin & Kustra, 2014).

This paper focuses on the development of a parallel FEM code for solving inverse problems that arise in the design of LDD process of tubes.

## 2. APPLIED RESEARCH METHODOLOGY

### 2.1. Model description

FEM code for modeling of the LDD process is based on the theory of plastic flow of incompressible material and the theory of non-stationary heat flow. In this approach the flow velocities, the mean stress and temperature are unknown. Boundary problem is described by the equations of theory of plasticity of non-compressible material in flow formulation and equation of non-steady state heat exchange. The developed numerical algorithms contain the solution of the following boundary-value problem:

Equilibrium equations:

$$\sigma_{ij,i} = 0\,, \tag{1}$$

compatibility condition:

$$\xi_{ij} = \frac{1}{2}\left(v_{i,j} + v_{j,i}\right), \tag{2}$$

constitutive equations:

$$\sigma_{ij}^{`} = \frac{2\overline{\sigma}}{3\overline{\xi}}\xi_{ij}\,, \tag{3}$$



incompressibility equation:

$$v_{i,j} = 0, \tag{4}$$

energy balance equation:

$$\rho c \dot{t} = k\left(t_{,i}\right)_{,i} + \beta \bar{\sigma} \bar{\xi} \tag{5}$$

and expression for flow stress:

$$\bar{\sigma} = \bar{\sigma}\left(\bar{\varepsilon}, \bar{\xi}, t\right), \tag{6}$$

where $\sigma_{ij}$ – stress tensor, $\xi_{ij}$ – strain rate tensor, $v_i$ – velocity component, $\sigma_{ij}^{`}$ – deviator of the stress tensor, $\bar{\sigma}, \bar{\varepsilon}, \bar{\xi}$ – effective stress, effective strain and effective strain-rate, respectively, t – temperature, $\beta$ – heat generation efficiency which is usually assumed as $\beta = 0.9\text{-}9.95$, k – thermal conductivity.

In equations (1)-(5) summation convention is used. Equations (1)-(4) were transformed into discrete form by means of virtual work-rate principle and finite element technique resulting in a non-linear system of algebraic equations where nodal values of velocity components and mean stress are considered as independent variables. Energy balance equation (5) is treated by means of Galerkin method. Iterative updating of heat generation and flow stress provides thermo-mechanical coupling of the problem. The mechanical boundary conditions involve stretching of the tube according to the scheme in figure 1. The thermal conditions for the contact with air are described by the convection law:

$$q_{air} = \alpha_{konw}\left(t - t_{\infty}\right), \tag{7}$$

and for heating zone are presented in the form of heat flux:

$$q_{laser} = k_a \frac{W}{S}, \tag{8}$$

where $W$ – laser power, $k_a$ – absorption coefficient of the laser, S – area of contact between laser and the tube, $\alpha_{konw}$ – coefficient of convective heat exchange with air, $t_{\infty}$ – temperature of environment. Value $k_a$ depends on the heated alloy, the optical surface condition of the material and area of laser beam contact with tube.

To solve the problem the 8 – node isoparametrical finite elements were used. The laser moving along a helical path of the impact area was considered (in fact, the tube was rotated relatively to the laser beam). FEM mesh with current localization of the laser beam (a) and resulting temperature distribution after 10 s of heating are shown in figure 2 (before elongation started).

As expression for flow stress (6) the equation of Hensel-Spittel (Hensel & Spittel, 1979) was used as the flow stress model:

$$\bar{\sigma} = A\exp\left(-m_1 t\right)\bar{\varepsilon}^{m_2}\bar{\xi}^{m_3}\exp\left(\frac{m_4}{\bar{\varepsilon}}\right)\left(1+\bar{\varepsilon}\right)^{m_5 t}$$
$$\exp\left(m_7\bar{\varepsilon}\right)\bar{\xi}^{m_8 t}t^{m_9} \tag{9}$$

The empirical coefficients $A$, $m_1$-$m_9$ proposed by Milenin et al (2014) are: $A$ = 330.833; $m_1$ = 0.00575295; $m_2$ = 0.127326; $m_3$ = 0.173357; $m_4$ = -0.00501432; $m_5$ = -0.00331755; $m_7$ = 0.5249617; $m_8$ = 0.000155541; $m_9$ = 0.180527.

The model of fracture, described in by Milenin and Kustra (2014), was implemented in the mechanical part of FE model. This model calculates the fracture parameter $\psi$, the value of which is equal to 1.0 at the moment of the fracture initiation.

### 2.2. Properties of stiffness matrix and used solver

The properties of the stiffness matrix for the mechanical problem only are described below These conditions for the heat transfer problem are be similar.

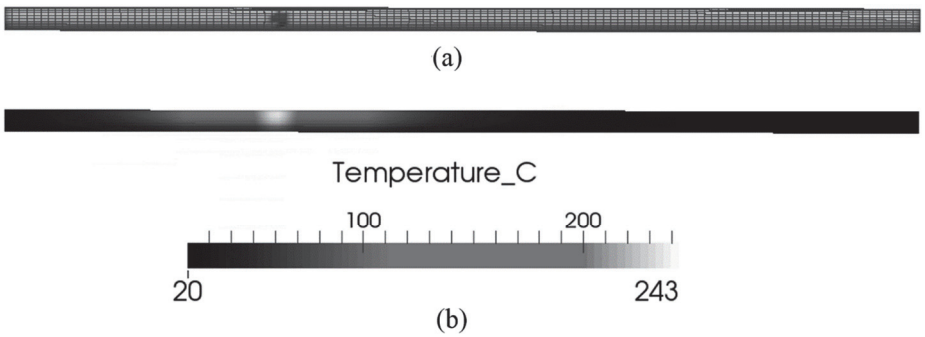


***Fig. 2.*** *FEM grid with current localization of the laser beam (a) and resulting temperature distribution after 10 s of heating (b).*



The 8 nodal velocity interpolation and constant value of mean stress in every finite element are used for solution of the mechanical flow problem. Thus, the size of the stiffness matrix of one element is 25 * 25 numbers. The global stiffness matrix after assembling is sparse. For grid chosen as an example in figure 2 (12288 nodes, 9155 elements, among 46019 Degrees of Freedom (DOF)) there is only 0.14% of the non-zero elements in the global stiffness matrix for mechanical problem (for thermal problem – 0.18%). The required memory for full stiffness matrix is DOF*DOF*8 = 16 941 986 888 byte = 17Gb. This is unacceptable value considering the need to solve multiple tasks simultaneously. Obviously, for such system of equations a solver for sparse matrix should be used. In this study PARDISO program (Schenk & Gärtner , 2004) was used. The following data have to be transmitted to solver:

Nonzero, int – the number of nonzero elements in stiffness matrix;

AK(Nonzero), real – nonzero values in a stiffness matrix;

JA(Nonzero), int – column indices. The number of column in the full stiffness matrix containing the non-zero values.

IA(DOF+1), int, – beginning of each row. IA(i) points to the first column index of row i in the array JA in compressed sparse row format , IA(DOF+1) = Nonzero + 1.

The process of solving the system of equations is very fast (less than a second for DOF = 46019), but the preparation of the above data requires much more time. Accordingly the reserve for increasing the speed of the solution is contained in optimizing the preparation of arrays AK, JA and IA. One of the key ideas of the proposed solution is to use the fact that for a single task arrays JA and IA remain constant at every time step. Thus, the task is to find quickly the position of the coefficients of global stiffness matrix in the linear array AK.

The proposed solution is to form a matrix of indexes IJ(DOF,DOF) containing an integer number of non-zero elements in AK array. For zero elements of stiffness matrix array IJ contains 0. Thus, it is possible to directly fill an array AK during assembling the elements. Memory of matrix IJ(DOF,DOF) for the described example is DOF*DOF*4 = 8 470 993 444 bytes, that is more than 8Gb. This is still a large amount of data, but it is filled once and does not change in the process of the solution. Essential is also the fact that it is possible to use the same copy of the array IJ by all the problems solved in the parallel mode. In that case, the proposed solution becomes more efficient both for parallel and for sequential solution of the tasks vector.

### 2.3. Parallelization

In the parallelization an advantage is made of the fact that the individual tasks have similar initial workpiece shape (it is always a tube) and they do not require remeshing (distortion of the elements is slight) are used. It causes that all tasks have FEM mesh with the same number of elements and nodes along the length and the thickness of the pipe. The identical element freedom tables for all grids guarantee the same position of non-zero elements in the global stiffness matrix. Therefore, arrays IA, JA, IJ for all tasks at all stages of the solutions will be the same and can be stored in a single copy. Thus, only the organization of the access to these data to all parallel processes is needed. OpenMP library (Chandra et al, 2001) is used to implement a parallel code. Scheme of code parallelization is shown in figure 3.

Parameters of tasks, that are solved in parallel mode, can be determined on the basis of any strategy. In this study to determine the calculation conditions the full factorial experimental design was used. In each task the sequential algorithm of calculation was used. That's way each task used only one processor and number of used processors is equal of number of tasks (NOT). The developed program automatically distributes the processors after generating the task vector. (Solvers 1–n on figure 3). An obvious problem may be the situation where the number of tasks is more than the number of available processors on the computer. In this case, the reduction in speedup is predictable.

## 3. THE RESULTS

The LDD process of tube made from MgCa08 alloy was considered. Initial outer pipe diameter was equal to 5 mm, internal was 4 mm. The models of the flow stress and the fracture described by Milenin et al (2010) were used in simulations. The scheme of full factorial experiment was used for generation of simulation variants. Varying factors were: velocity of the tube relative to the laser ($V_2$ in figure 1b) and tube elongation rate $dV = V_1 - V_2$ (figure 1b). Conditions and selected results of numerical experiments are presented in the table 1.



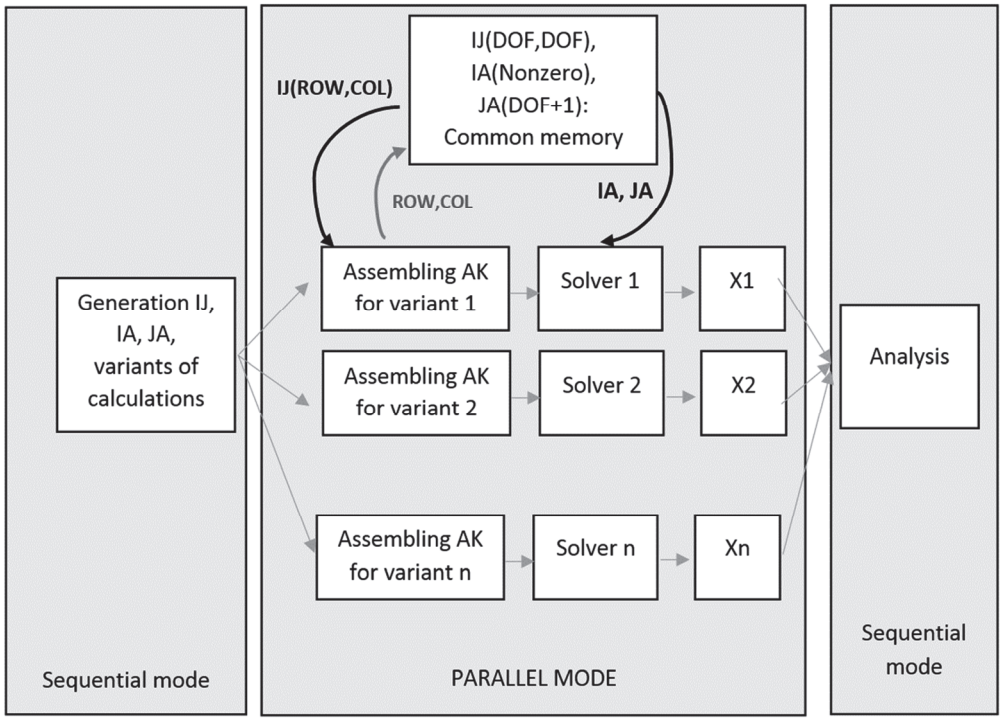


**Fig. 3.** *Algorithm of parallelization, X1, X2, ..., Xn – solution of tasks.*

***Table 1.*** *Conditions and results of a numerical experiment*

| | $V_2$ mm/s | $dV$ mm/s | $T_{max}$ °C | $D_{out}$ mm | $D_{in}$ mm | Ψ |
|---|---|---|---|---|---|---|
| 1 | 0.2 | 0.3 | 452 | 2.105 | 1.710 | 0.46 |
| 2 | 0.5 | 0.3 | 406 | 3.851 | 3.094 | 0.18 |
| 3 | 0.8 | 0.3 | 375 | 4.236 | 3.397 | 0.132 |
| 4 | 1.1 | 0.3 | 355 | 4.351 | 3.486 | 0.189 |
| 5 | 0.2 | 0.5 | 496 | - | - | >1 |
| 6 | 0.5 | 0.5 | 425 | 3.095 | 2.498 | 0.366 |
| 7 | 0.8 | 0.5 | 393 | 3.769 | 3.029 | 0.251 |
| 8 | 1.1 | 0.5 | 369 | 3.987 | 3.197 | 0.362 |
| 9 | 0.2 | 0.7 | 518 | - | - | >1 |
| 10 | 0.5 | 0.7 | 430 | - | - | >1 |
| 11 | 0.8 | 0.7 | 404 | 3.233 | 2.606 | 0.416 |
| 12 | 1.1 | 0.7 | 376 | 3.672 | 2.950 | 0.538 |

The obtained results allow to choose the parameters of the process in order to obtain a predetermined tube diameter. It is shown that the increase of speed $V_2$ increases the final diameter of the tube at the same rate of stretching of the pipe. This happens due to the fact that the temperature field changes in the deformation zone. Effect of tube stretching speed is quite obvious - with an increase in this parameter decreases the diameter of the pipe. Thus, it is possible to obtain the desired geometric dimensions of the finished pipe by selecting the velocity values $V_1$, $V_2$.

It is essential to limit at the range of process parameters according to the condition of absence of fracture. The destruction of the pipe is obtained for the variants 5, 9 and 10 shown in the table 1. Destruction occurs by the mechanism of the formation of the neck. The reason of strain localization is associated with metal overheating to temperatures above 400 C. The high value of temperature does not influence the strain localization directly (high temperature increases ductility), but increases the gradient of temperature in direction of the length of the pipe in the deformation zone which provides strain gradient and formation of the neck.

The initial stage of neck forming and increasing the fracture parameter ψ is shown in figure 4 for variant 9.

Thus, the model allows to determine not only the parameters needed to obtain required tube diameter, but also to predict the allowable window of process parameters. Model also allows to explore the non-uniformity of the diameter along the tube. An example of such non-uniformity can be observed at the boundary of the permissible window of technological parameters, eg. for the variant 1. The tube diameter distribution for this variant is shown in figure 5. Thus, on the border of the window of possible technological parameters instability of the process and the unevenness of the tube diameter increases, although it does not lead to fracture. In the region of a stable process (for example variant 2) the unevenness of the diameter is minimal (figure 6).



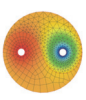

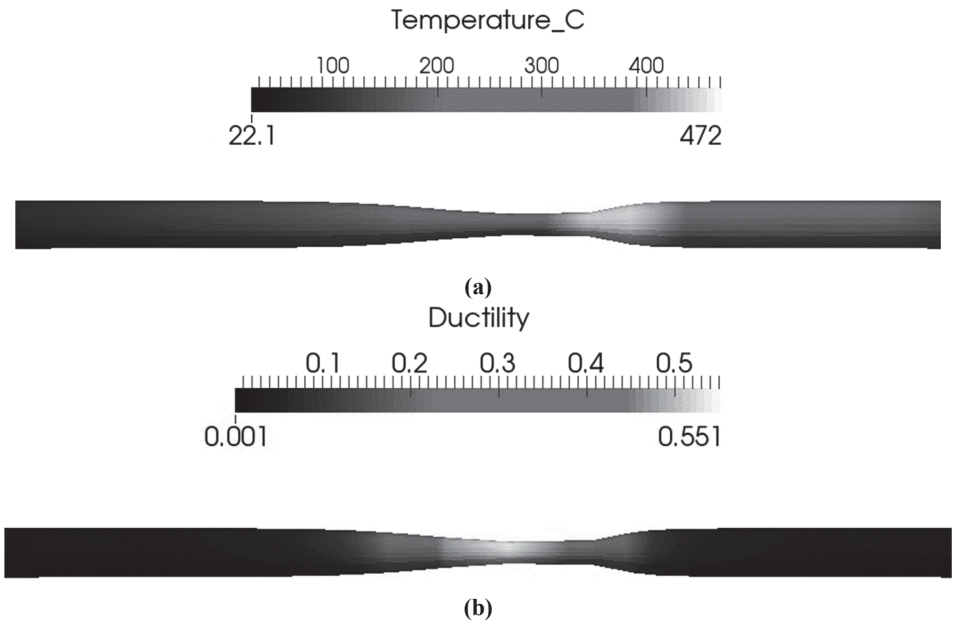


***Fig.4.*** *Distribution of temperature (a) and ductility parameter* $\Psi$ *(b) at the moment of initial localization of deformation in the neck zone, variant 9 in the table 1.*

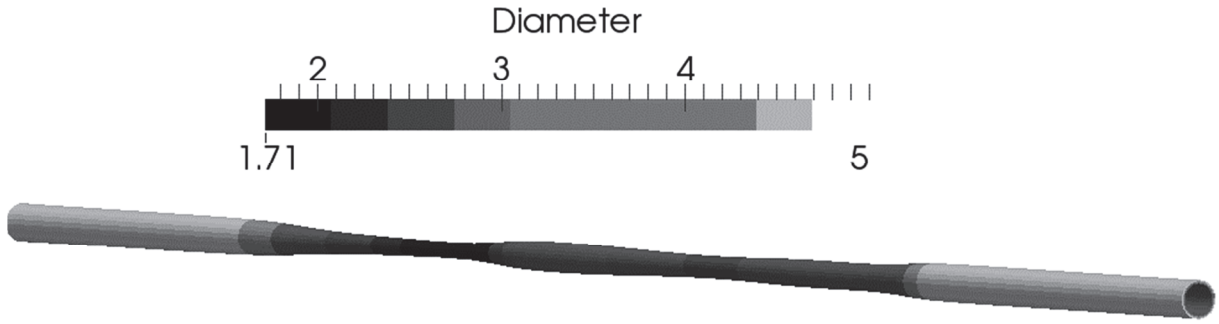


***Fig. 5.*** *Non-uniform distribution of the tube diameter after deformation in the unstable mode (variant 1 in the table 1).*

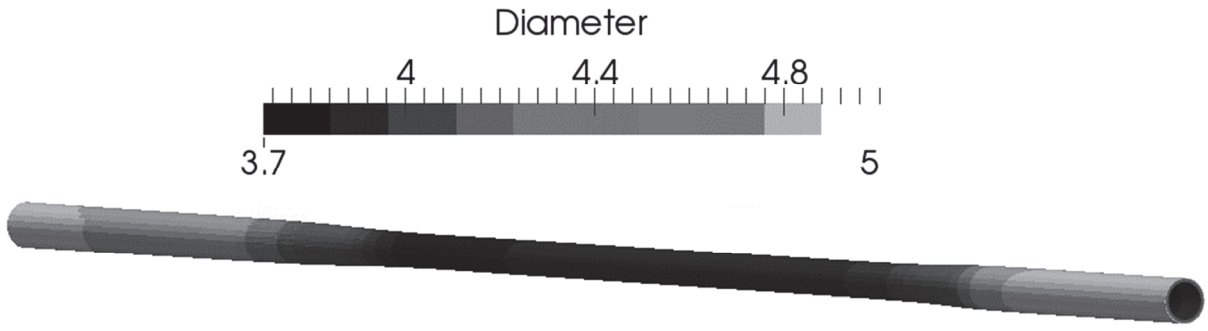


***Fig. 6.*** *Uniform distribution of the tube diameter after deformation in the stable mode (variant 2 in the table 1).*

The distribution of the estimated outside diameter of the pipe as a function of $V_2$ and $dV$ is shown in figure 7. This distribution shows that it is possible to achieve a given external diameter using different combinations of factors. For example, the diameter of 4.0 mm can be obtained with $V_2$ = 0.6 mm/s and $dV$ = 0.3 mm/s or $V_2$ = 0.9 mm/s and $dV$ = 0.45 mm/s. It allows to take into account additional conditions, for example, try to achieve a given internal diameter or minimize the difference in diameters along the tube. The range of permissible values of factors is limited by the line $D_{out}$ = 3.0 mm, above which the destruction of the material or instability of the process is likely to happen.



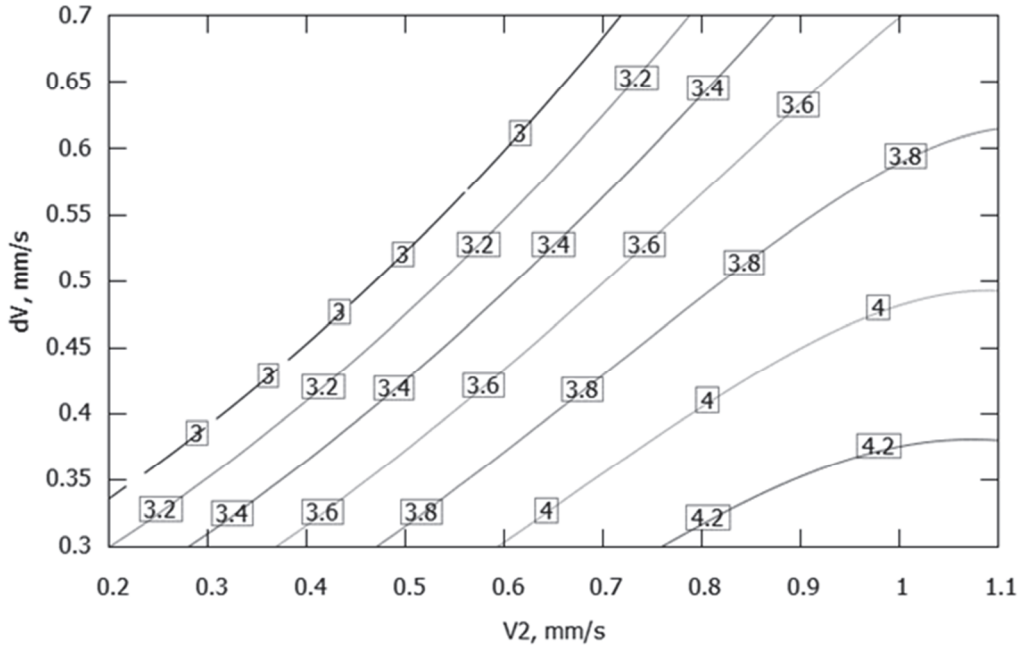


***Fig. 7.*** *Dependence of the outer diameter of final tube on parameters $V_2$ and dV.*

## 4. EFFECTIVENESS OF THE PARALLEL PROGRAM

In the developed code acceleration of calculations is achieved in two independent ways. First is based on one calculation of matrix of indexes IJ(DOF,DOF) for all tasks. The effectiveness of this method depends on the relationship between the time of calculating the matrix of indices IJ $\tau_m$ and the time of one solution of FEM $\tau_S$.

For conventional sequential computations, the calculating time is $\tau = NOT(\tau_m + \tau_S)$. But if the proposed algorithm is used, this value becomes equal to $\tau = \tau_m + NOT\tau_S$. Therefore, speedup$_1$ can be calculated from equation:

$$speedup_1 = \frac{\tau_m + \tau_S}{\frac{\tau_m}{NOT} + \tau_S} \qquad (10)$$

The value of speedup1 depend on DOF, NOT and conditions of simulations (physical process time). Estimated speedup1 for NOT=16 is changed from 1.2 (DOF=9927) to 5.5 (DOF=91323).

The second way of accelerating computing is based on parallelization of calculations. To evaluate the efficiency of parallel computations, a comparison was made between parallel and sequential modes. For the analysis, two FEM models with different DOF were chosen. Model 1 matched the DOF=9927, model 2 – DOF=45627.

During calculation the number of tasks variated from 1 to 22. Each task was allocated at one processor. The calculations were performed on a computer with number of processors (p) 16. The FEM code was tested in two modes – parallel and sequential. The sequential solution was based on the same algorithm as the parallel algorithm, but the FEM tasks were solved sequentially. The results of speedup2 measurement is present on figure 8. For sequential mode the dependence between time and NOT is linear for all range of NOT. However for parallel mode this dependence is not linear. Time of solution in parallel mode significantly increased for NOT>p and became more than time of sequential solution (speedup2<1). As follows from the graphs in the

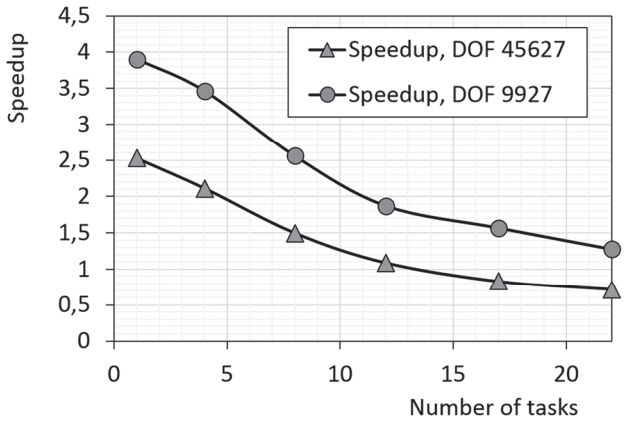


***Fig. 8.*** *Dependence between speedup$_2$ and number of tasks in parallel mode.*

figure 8, the proposed model and the method of its parallelization are much more effective for NOT<0,7-0,9p. In this range of NOT the speedup2 is approximately 2-4. For larger NOP values, it is more



efficient to use a sequential mode or to divide the problem into smaller parts.

## 5. CONCLUSIONS

1. The developed FEM code was designed to solve inverse problems in developing the technology of laser dieless drawing. Code is based on the application of the parallel computing. The numerical efficiency of the code is based on simultaneous using by all tasks the common matrix of addresses of non-zero elements in the stiffness matrix.
2. The developed program in parallel mode is more effective for number of tasks late than 0,7-0,9 of the number of available processors.
3. An example of process analysis, in which the stable process and the destruction of a tube during laser dieless drawing process was predicted, was shown in the paper.

## ACKNOWLEDGEMENTS

Financial assistance from the NCBiR of Poland, Project No. V4-Jap/2/2016 is acknowledged.

## REFERENCES

Chandra, R., Menon, R., Dagum, L., Kohr, D., Maydan, D., McDonald, J., 2001, *Parallel Programming in OpenMP*, Morgan Kaufmann.

Furushima, T., Manabe, K., 2007, Experimental and numerical study on deformation behavior in dieless drawing process of superplastic microtubes, *Journal of Materials Processing Technology*, 191, 59-63.

Furushima, T., Masuda, T., Manabe, K., Alexandrov, S., 2011, Prediction of Free Surface Roughening by 2D and 3D Model Considering Material Inhomogeneity, *Journal of Solid Mechanics and Materials Engineering,* 5, 12, 978-990.

Furushima, T., Imagawa, Y., Furusawa, S., Manabe, K., 2015, Development of rotary laser dieless drawing apparatus for metal microtubes, *Key Engineering Materials*, 626, 372-376.

Furushima, T., Imagawa, Y., Furusawa, S., Manabe, K., 2014, Deformation profile in rotary laser dieless drawing process for metal microtubes, *Procedia Engineering*, 81, 700-705.

Hensel, A., Spittel, T., 1979, *Kraft- und Arbeitsbedarf Bildsomer Formgeburgs Verfahren*, VEB Deutscher Verlag fur Grundstoffindustrie, Lipsk (in German).

Kustra, P., Milenin, A., Płonka, B., Furushima, T., 2016, Production process of biocompatible magnesium alloy tubes using extrusion and dieless drawing processes, *Journal of Materials Engineering and Performance*, 25/6, 2528-2535.

Li, Y., Quick, N. R., Kar, A., 2002, Dieless laser drawing of fine metal wires, *Journal of Materials Processing Technology,* 123, 451-458.

Milenin, A., Kustra, P., Byrska-Wójcik, D., Furushima, T., 2017, Physical and Numerical Modelling of Laser Dieless Drawing Process of Tubes from Magnesium Alloy, *Procedia Engineering*, 207, 2352-2357.

Milenin, A., Kustra, P., 2014, Optimization of profile extrusion processes using the finite element method and distributed computing, *eScience on distributed computing infrastructure: achievements of PLGrid Plus domain-specific services and tools,* eds. Bubak, M., Kitowski, J., Wiatr, K., Springer International Publishing, 378-390.

Milenin, A., Gzyl, M., Rec, T., Plonka, B., 2014, Computer aided design of wires extrusion from biocompatible Mg-Ca magnesium alloy, *Archives of Metallurgy and Materials,* 59, 551-556.

Milenin, A., Kustra, P., Paćko M., 2010, Mathematical model of warm drawing of MgCa0.8 alloy accounting for ductility of the material, *Computer Methods in Materials Science*, 10, 69-79.

Schenk, O., Gärtner K., 2004, Solving unsymmetric sparse systems of linear equations with PARDISO, *Future Generation Computer Systems*, 20, 475-487.

Tiernan, P., Hillery, M.T., 2004, Dieless wire drawing - an experimental and numerical analysis, *Journal of Materials Processing Technology*, 155-156, 1178-1183.

## RÓWNOLEGŁY KOD MES DO SYMULACJI PROCESU LASEROWEGO BEZ NARZĘDZIOWEGO CIĄGNIENIA RUR

Streszczenie

Artykuł jest poświęcony opracowaniu kodu MES do symulacji procesu laserowego bez narzędziowego ciągnienia mikro rur ze stopu magnezu. Trudności wyznaczenia parametrów tej technologii są związane z faktem, że rozpatrywany proces jest oparty o swobodne odkształcenie wsadu. Z tego powodu wyznaczenie parametrów, które pozwalają otrzymać zadane wymiary rury, jest trudne. Proponowane rozwiązanie wykorzystuje obliczenia równolegle. Rozpatrzono równoległe rozwiązanie wektora zagadnień, które są wygenerowane na podstawie teorii eksperymentu czynnikowego. Rozwiązane zadania pozwalają na wygenerowanie okna dopuszczalnych parametrów procesu i wyznaczenie parametrów, które gwarantują zadane wymiary rury. Numeryczna wydajność opracowanego kodu jest oparta o wykorzystanie przez wszystkie równolegle procesy jednej macierzy zawierającej położenie nie zerowych elementów macierzy sztywności..

*Received: March 8, 2017*
*Received in a revised form: July 21, 2017*
*Accepted: November 30, 2017*